J. Mater. Environ. Sci. 7 (3) (2016) 871-877
ISSN : 2028-2508
CODEN: JMESCN

Impedance spectroscopy characterization of $Pb_{0.96}La_{0.04}Fe_{0.03}Ti_{0.97}O_3$ nano-ceramics for negative coefficient thermistor (NCT)

L. H. Omari[1,4*], S. Sayouri[1], T. Lamcharfi[2], L. Hajji[3], M. Haddad[4], H. Lemziouka[5]

[1] *LPTA, Department of Physics, Faculty of Sciences-DM, B.P. 1796, Fez-Atlas, Morocco*
[2] *LSSC Department Electrical Engineering, FST, Route d'Immouzer, Fez, Morocco*
[3] *Department of Physics, Faculty of Sciences and Technics gueliz Marrakech, Morocco*
[4] *LASMAR Department of Physics, Faculty of Sciences, Meknes Zitoune, Morocco*
[5] *LPTA, Department of Physics, Faculty of Sciences, Aïn Chock, Casablanca, Morocco*
[*] *Corresponding author. E-mail: Tel: +212669164585*

Received 28 Feb 2015, Revised 04 Oct 2015, Accepted 06 Oct 2015,
**Corresponding author: E-mail: bophysiq@gmail.com*

Abstract
Nano-ceramic $Pb_{0.96}La_{0.04}Fe_{0.03}Ti_{0.97}O_3$ (PL4F3T) was prepared by Sol-Gel reaction method. Raman and XRD patterns of PL4F3T ceramic showed that a single-phase was formed exhibiting a pseudo-cubic crystal structure. With SEM, we examined the micro-structural properties. The electrical behavior was investigated by the impedance spectroscopy in the range of 50°C - 600°C. This study was carried out by analysis of the complex impedance (Z*) from the measurement range of 1 kHz to 1 MHz. Complex analysis provides wider information related to charge transport processes.

Key words: Ferroelectrics, Sol-Gel process, Complex impedance analysis, Non Debye relaxation, Nyquist plots.

1. Introduction
Lead titanate ($PbTiO_3$ or PT) belongs to a most important perovskite family due to its remarkable ferroelectric and piezoelectric features in polycrystalline form [1-3]. It exhibits a single transition from para-electric with cubic phase to ferroelectric with tetragonal phase [4]. The substitution of any suitable ions at the Pb and/or Ti site of PT results in substantial modification in their electrical properties so as to make them suitable for a wide variety of industrial applications. The charge transport can take place via mode such as dipole reorientation, charge displacement and space charge formalism [5]. Fluctuation of the oxidation state of these ions results in the formation of oxygen ion vacancies which causes thermally activated conduction. Thus most of the multi-ferroïc materials show high leakage current and low ferroelectric polarization [6]. In order to improve the ferroelectric properties, lanthanum (La) has been introduced. An appropriate and optimum amount of La lowers the leakage current, which is a primary requirement for non-volatile random access memory (NVRAM) applications [7]. Sol-Gel process has been used to synthesize nano-crystalline ferroelectrics. It was shown that the crystallization of PL4F3T occurred at 700°C, which temperature is inferior to that reported for the same composition prepared by the traditional solid-state reaction technique [8]. Complex impedance spectroscopy (CIS) is a well-established method to investigate electrical properties of materials. It describes the electrical processes occurring in a system on application of an ac signal as input perturbation [9-11]. It has great ability to analyze the relaxation phenomenon occurring in the material, whose time constants range over several orders of magnitude [12]. A much more profound analysis is possible by combining the impedance analysis with use of the complex electrical formalism [13].
The aim of this work is to study the mechanism of electrical properties of electro-ceramics materials, synthesized by sol-gel route, using complex impedance spectroscopy (CIS) for high capacitance capacitor, high performance sensor and negative coefficient thermistor (NCT). The technique ensures separation among the bulk, grain, grain boundaries and electrolyte interface properties. It has great ability to analyze the relaxation phenomenon occurring in the material and whose time constants range over several orders of magnitude.

2. Materials and methods

The details of experiment used in this work were published elsewhere [14]. In fact, the La^{3+}/Fe^{3+} modified lead titanate (PL4F3T) was synthesized from high purity precursors by a Sol-Gel reaction method [14]. Then, the powder was calcined at optimized temperature (700 °C) and time (2h) in a programmable oven. The formation of single-phase compound was confirmed by XRD. The calcined powders were uni-axially pressed to fabricate the pellets as a capacitance and sintered at 1100°C for 2h. The electrical measurement was carried out at an input signal level of 1V in a wide temperature range of (50°C - 600°C) using a computer controlled impedance analyzer, in the frequency range of 1kHz to 1MHz.

3. Results and discussion

Fig.1 shows the X-ray diffraction patterns collected at room temperature of PL4F3T powder. All the lattice parameters were determined, using a computer program (Cell-Ref). The sample crystallized completely without the presence of peaks corresponding to the reactant oxides or any other secondary phases, and exhibited a patterns characteristic of a single-phase compound that has a pseudo-cubic (tetragonal structure with c/a close to 1.0104) structure with the space group Pm-3m. This finding is consistent with our previous work [14], which demonstrates that the crystallization process occurred between 400 and 500 °C. The lattice parameters and volume cell were estimated and resumed in the table 1. The average grain sizes determined from the analysis of the XRD patterns, using Scherer formula [15]. The average crystallite size (C.S) is of the order of several tens of nanometers, suggesting that the sample has a nanometric scale.

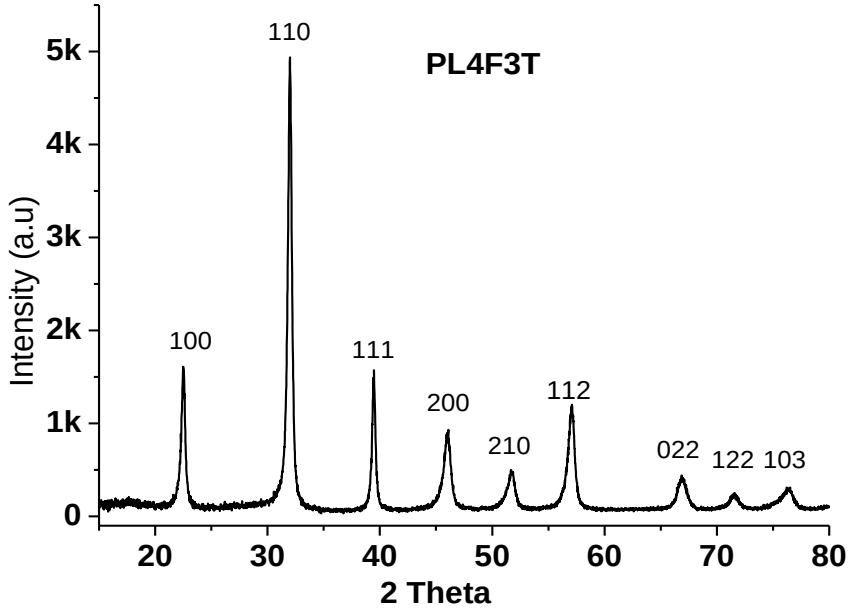

Figure 1: XRD pattern of PL4F3T powder calcined at 700°C (2h).

Table 1: Physical properties of PL4F3T

	a (Å)	c (Å)	V(Å^3)	C.S. (nm)	T_m (1kHz)	ε_m (1kHz)	E_{atc} (eV)	f_o (kHz)
PL4F3T	3,936	3,977	61,627	33,25656	374.2 °C	6061.98	0,4116	$4{,}98.10^8$

This sample was also analyzed by Raman spectroscopy to characterize the tetragonal phase structure. The spectrum of the PL4F3T in Fig. 2 shows its usual profile, with well-defined characteristic peaks as reported in literature [16]. Because of Raman scattering spectroscopy is a quite sensitive tool for local distortion, much more than XRD [17], it can be used to evaluate how the rare earth ion (Yb^{3+} or Eu^{3+}) affects the crystal structure of the host material [18]. Some authors affirm that there is dependence between the particle size and the Raman shift [16]. Therefore, we can ascribe the Raman modes shifting only to the influence of the lanthanum on the tetragonality. The Raman spectra show that the structure is not really cubic and confirms the tetragonal structure type.

SEM micrograph (Fig.3) indicates the microstructure of the sample with fine, homogeneous and spherical grains which a sign of the best density of the compound. From this micrograph, the average grains size (G.S) is evaluated around nano-metric scale of 200 nm.

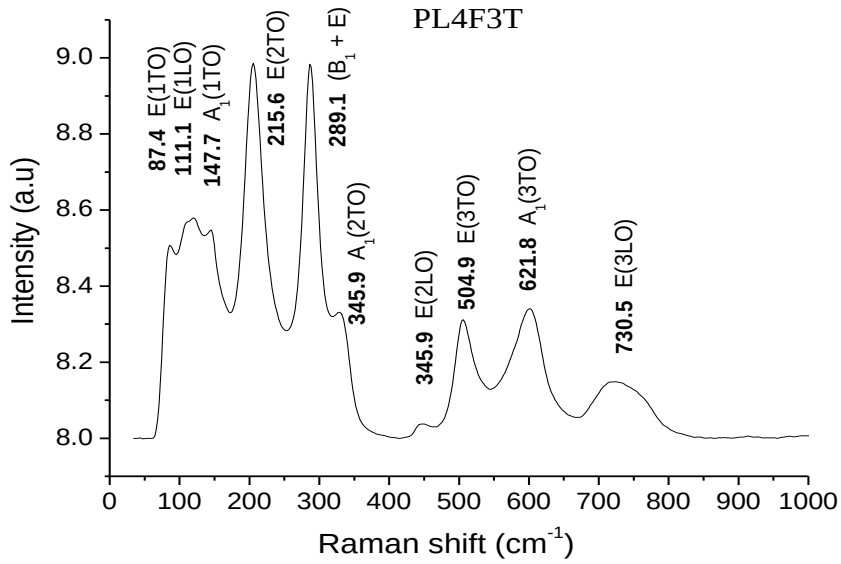

Figure 2: Raman spectra of PL4F3T powder calcined at 700°C (2h).

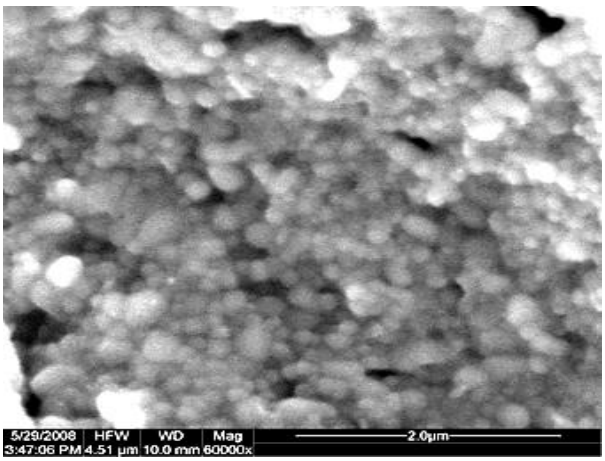

Figure 3: SEM Micrograph of PL4F3T powder calcined at 700°C (2h).

The temperature dependence of the dielectric constant and dielectric loss of the PL4F3T specimen at different frequencies are shown in Fig. 4a and Fig. 4b respectively. The dielectric constant shows a peak at T_m = 374.2 °C. The broadening of this peak increases with the increases in frequency from 1 kHz to 600 kHz, allowed that PL4F3 present a diffuse phase transition. We can note that the values of the losses tan(δ) are very low (tan(δ)=0,118 at 1 kHz and at room temperature 35.26 °C).

Electrical behavior of the compound is characterized over a wide temperature and frequency range by using AC impedance methods as semi-empirical complex Cole–Cole equation. Data are analyzed in terms of four possible complex formalisms, the impedance Z^*, the electrical modulus M^*, the admittance Y^* (or A^*) and the permittivity (ε^*) [19].

Each one of these parameters is related to another according to the expressions [20]:

$$M^* = \omega C_0 Z^* \quad \text{Eq.(1)}$$

$$\varepsilon^* = \frac{1}{M^*} \quad \text{Eq.(2)}$$

$$\frac{1}{Z^*} = Y^* = j\omega C_0 \varepsilon^* \quad \text{Eq.(3)}$$

$$Z^* = Z' - iZ'' = R - \frac{1}{j\omega C} \quad \text{Eq.(4)}$$

where ω (=2πf) is the angular frequency,

$$C_0 = \frac{\varepsilon_0 S}{e} \quad \text{Eq.(5)}$$

is the vacuum capacitance of the measuring cell. With e (1mm) and S (113 mm^2) are respectively electrodes spacing and surface. The use of the function M^* or ε^* is suitable for the resistive and/or capacitive analysis when localized relaxation dominates while the Z^* or Y^* functions are appropriate when the long-range conductivity is dominate. Especially the use of Z^* formalism allows for a direct separation of the bulk, grain boundary and electrode contributions to the phenomena, and lead to the determination of each individual resistance [21]. From this formalism the electric loss is:

$$\tan(\delta) = \frac{\varepsilon''}{\varepsilon'} = \frac{M''}{M'} = \frac{Z'}{Z''} = \frac{Y'}{Y''} \qquad \text{Eq.(6)}$$

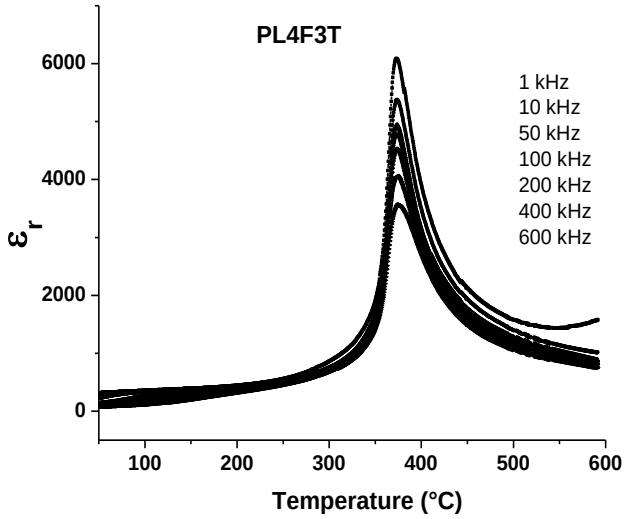

Figure 4a: Permittivity as a function of temperature at different frequencies.

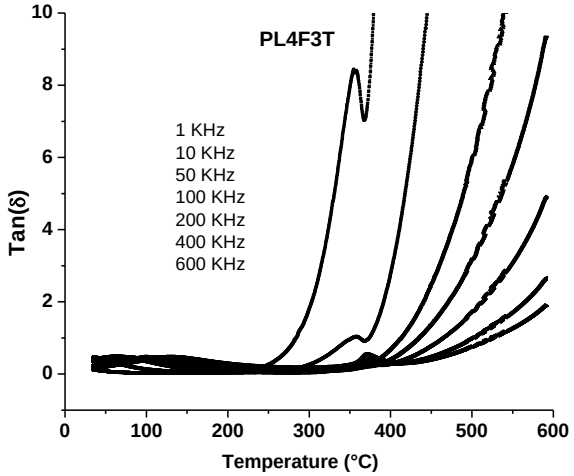

Figure 4b: Loss spectra as a function of temperature at different frequencies.

Thus, this study may be performed on the (ε', ε"), (Z', Z"), (M', M") or (Y', Y"). We focuses our study on Z' and Z'' evolutions on frequency at various temperatures. Fig.5a shows complex impedance spectra (Nyquist plots) for PL4F3T ceramic over a wide range of temperature. However, the effect of temperature on impedance behavior is more apparent at higher temperatures ($T > T_m$). The pattern of impedance spectrum is characterized by the presence of semicircular arcs at different temperatures (Fig.5a). This may possibly be attributed to the presence of single electrical relaxation phenomena [22] in the material under investigation. The radius of the semicircular arc increases with increasing temperature to reach a maximum in T_m and after that, it decreases as temperature increases. The intercept of semicircular arc with the real axis gives an estimate of sample resistance. Each semicircle represents the contribution of a particular process (electrodes and contacts, grain boundaries, grain interior) to the total impedance of the sample. Measured values in the form of Nyquist plots are rarely ideal semicircular. Most of the authors describe them as depressed semicircle with their center lying

below the x-axis. This phenomenon is called non-Debye relaxation [23]. Thus in our investigation we can describe that PL4F3T reveal a non-Debye relaxation. The decrease of radii of the semi-circular curves, for $T>T_m$, with the increase in temperature indicates that the bulk resistance decreases and the bulk conductivity increases which is analogous to the negative temperature coefficient of resistance (NTCR) property.

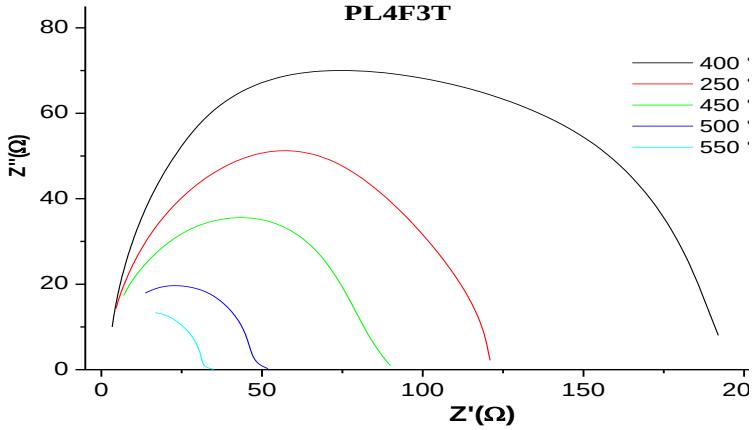

Figure 5a: Nyquist plots of complex impedance at various temperatures.

In addition, Fig.5b shows the variation of real part of impedance (Z') as a function of frequency over a wide range of temperature. The nature of variation shows a monotonous decrease in the value of Z' with rise in the frequency.

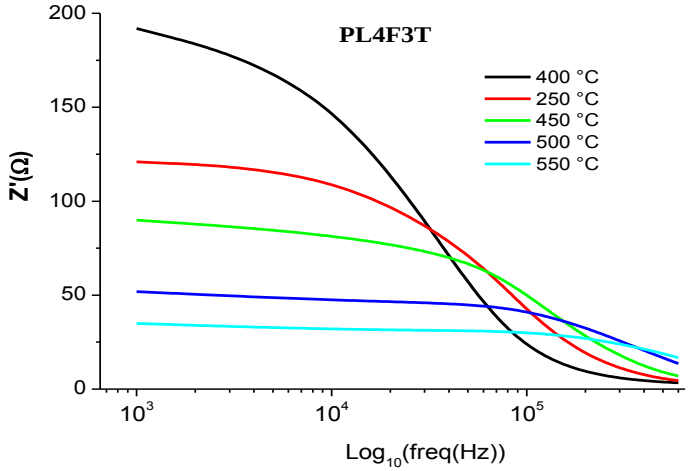

Fig. 5b: Real and imaginary parts of complex impedance as function of frequency.

For $T>T_m$ the impedance value is higher at lower temperatures in the low frequency region and decreases gradually with increase in frequency. This observation may possibly be related to a lack of restoring force governing the mobility of charge carriers under the action of an induced electric field at higher temperatures. The merger of real part of impedance (Z') in the higher frequency domain for all temperatures indicates a possibility of the release of space charge as a result of lowering in the barrier properties of the material [24,25]. Moreover, Fig.5c shows the variation of the imaginary part of the impedance with frequency (i.e., loss spectrum) at different temperature. A peak has been observed which further broadened with rise in temperature. The trend of variation of ε'' with frequency is typical of the presence of electrical relaxation phenomena in the material. The asymmetric broadening of the peaks suggests the presence of electrical process in the material with a spread of relaxation time [26]. The higher frequency side of the Z'' peak represents the range of frequencies in which the ions are spatially confined to their potential wells and the ions can make only short-range motion within the well [27,28]. The region where peak occurs is indicative of the transition from long-range to short-range mobility with increase in frequency.

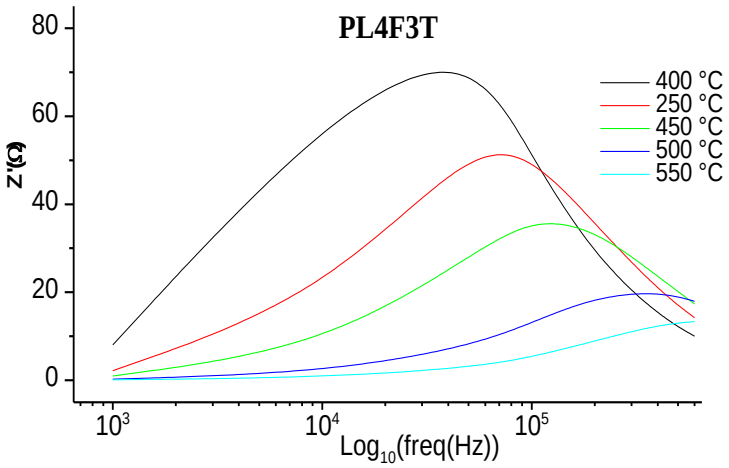

Figure 5c: Frequency dependence of imaginary parts of complex impedance at various temperatures.

In a relaxation system, the conduction relaxation time (τ_c) can be estimated from Z'' versus log (f) plot (Fig.6) using the relation: $\tau_c = 2\pi/\omega = 1/f_{max}$ where f_{max} is the relaxation frequency. Using a nonlinear fitting method, the experimental data can be well fitted by the Debye peak with a distribution in relaxation time and an exponential background [29,30]. The activation energy can be deduced from the Arrhenius law [31]:

$$f_{max} = f_0 exp\left(\frac{E_a\,\tau_c}{K_B T}\right) \qquad \text{Eq.(7)}$$

where f_0 is the pre-exponential factor, k_B is the Boltzmann constant and T is the absolute temperature. It is observed that the value of f_{max} decreases with increase of temperature, which is a typical semiconductor behavior. Fig.6 describes the linear relationship between the log(f_{max}) and inverse temperature (1/T).

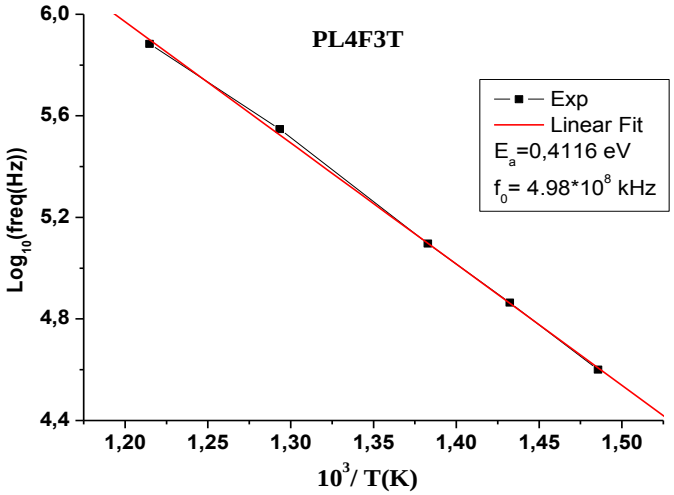

Figure 6: Variation of relaxation time with the inverse of temperature.

From this figure, the relaxation parameters f_0 and the activation energy $E_{a\tau c}$ were evaluated in the table 1. The $E_{a\tau c}$ is close to that for the diffusion of oxygen ions, suggesting that the dielectric relaxation process is associated with oxygen ion diffusion.

Conclusions

In summary, we synthesized the PL4F3T ceramics, using sol-gel reaction route. On the basis of the Arrhenius law, complex impedance formalism, we studied the effect of the temperature and frequency on to the dielectric properties and frequency relaxation times and estimated the activity energy value. Moreover, the decrease of radii of the semi-circular curves, for T>Tm, with the increase in temperature notify that the bulk resistance decrease and the bulk conductivity increase which is analogous to the negative temperature coefficient of resistance (NTCR) property. The form of Nyquist plots indicate that PL4F3T reveal a non-Debye relaxation. From the value of $E_{a\tau c}$, dielectric relaxation process is associated with oxygen ion diffusion.

Acknowledgements-I dedicate this work to the spirit of Pr. Abdalmajid Yacoubi, who strongly supported me while he was alive. God's mercy.

References

1. Chandler C. D., Roger C. and Hampden-Smith, M. *J., Chem. Rev*. 93, (1993) 1205-1241.
2. Pramanik N. C., Anisha N., Abraham P. A., RaniPanicker N., *J. Alloys. Compd*. 476, (2009) 524-528.
3. Bhella A. S., Guo R., Roy R., *Mater. Res. Innov*. 4, (2000) 3-26.
4. Sheng G., Zhang J. X., Li Y. L., Choudhury S., Jia Q. X., Liu Z. K., Chen L. Q., *J. Appl. Phys.* 104, (2008) 054105.
5. Sen S., Choudhary R. N. P., Tarafdar A., Pramanik P., *J. Appl. Phys*. 99, (2006) 124114/1-8.
6. Palkar V. R., John J., Pinto R., *Appl. Phys. Lett.* 80, (2002) 1628-1630.
7. Venkateswarlu P., Laha A., Krupanidhini S. B., *Thin Solid Films* 474, (2005) 1.
8. Shukla A., Choudhary R. N. P., Thakur A. K., *J. Mater. Sci. - Mater. Electron.,* 20 (8), (2009) 745-755.
9. Pradhan D. K., Samantray B. K., Choudhary R. N. P., *Mater. Sci. Engg. B.* 116, (2005) 7-13,.
10. Barick B. K., Choudhary R. N. P., Pradhan D. K., *Ceramics International* 39, 5, (2013) 5695-5704.
11. Ortega N., Kumar A., Bhattacharya P., Majumder S. B., Katiyar R. S., *Phys. Rev. B* 77, (2008) 014111.
12. Raymonds O., Font R., Portelles J., Siqueiros J. M., *J. Appl. Phys.*, 97, (2005) 084108.
13. Sinclair D. C., West A. R., *J. Appl. Phys.* 66, (1989) 3850.
14. Omari L. H., Sayouri S., the book of «Élaboration et Caractérisation de Céramique PbLaFeTiO3», *Edition EUE* (ISBN 978-3-8417-8255-7; 2011) p. 67-69.
15. Cullity B. D., Elements of X.R.D., 2ed. *Philippines (Addison-Wesley, 1978)* p. 278-281.
16. Miryam R. J., Barba-Ortega J., Pizani P. S., *J. Appl. Phys.* 113, 013512 (2013)
17. Tornberg N. E., Perry C. H., *J. Chem. Phys*. 53, (1970) 2946–2955.
18. Shi Y., Yajie L., Dechao Y., Zhongmin Y., Qinyuan Z., *J. Appl. Phys.*, 110, (2011) 013517
19. Gurevich V. M., Electrical Conductivity of Ferroelectrics (*Moscow, 1969*) p. 383.
20. Abram E. J., Sinclair D. C., West A. R., *J. Electroceram*. 10,(2003) 165-177.
21. Tomozawa M., Cordaro J., Singh M., *J. Mater. Sci.* 14, (1979) 1945-1951.
22. Hodge I. M., Ingram M. D., West A. R., *J. Electroanal. Chem*. 74, (1976) 125-143.
23. John T., Irvine S., Derek Dr., Sinclair C., Anthony R. West, *Adv. Mater*. 2, (1990) 132-138.
24. Archana S., Choudhary R. N. P., Thakur A. K., *J. Mater. Sci. - Mater. Electron*., 20, (2009) 745- 755.
25. Behera B., Nayak P., Choudhary R. N. P., *J. Alloys Compd.* 436, (2007) 226-232.
26. Joachim M., *Solid State Ionics* 157, (2003) 327-334.
27. Bharati R., Singh R. A., Wanklyn B. M., *J. Mater. Sci.* 16, (1981) 775-779.
28. Archana S., Choudhary R. N. P., *Current Applied Physics* 11, (2011) 414-422.
29. Nobre M. A. L., Langfredi S. J., *Journal of Physics and Chemistry of Solids* 62, (2001) 1999-2006.
30. Archana S., Choudhary R. N. P., *Physica B: Condens. Matter* 406, (2011) 2492-2500.
31. Kingery W. D., Bowen H. K., Uhlmann D. R., Introduction to Ceramics 2nd Ed. (*Wiley, 1976*) New York p. 647-651.